BIOCHEMISTRY
including biophysical chemistry & molecular biology

Article

pubs.acs.org/biochemistry

Properties of the Mechanosensitive Channel MscS Pore Revealed by Tryptophan Scanning Mutagenesis

Tim Rasmussen,[†] Akiko Rasmussen,[†] Shivani Singh,[†,§] Heloisa Galbiati,[†] Michelle D. Edwards,[†] Samantha Miller,[†] and Ian R. Booth*[,†,‡]

[†]School of Medical Sciences, University of Aberdeen, Foresterhill, Aberdeen AB25 2ZD, United Kingdom

[‡]Division of Biology and Biological Engineering, California Institute of Technology, 1200 East California Boulevard, Pasadena, California 91125, United States

Supporting Information

ABSTRACT: Bacterial mechanosensitive channels gate when the transmembrane turgor rises to levels that compromise the structural integrity of the cell wall. Gating creates a transient large diameter pore that allows hydrated solutes to pass from the cytoplasm at rates close to those of diffusion. In the closed conformation, the channel limits transmembrane solute movement, even that of protons. In the MscS crystal structure (Protein Data Bank entry 2oau), a narrow, hydrophobic opening is visible in the crystal structure, and it has been proposed that a vapor lock created by the hydrophobic seals, L105 and L109, is the barrier to water and ions. Tryptophan scanning mutagenesis has proven to be a highly valuable tool for the analysis of channel structure. Here Trp residues were introduced along the pore-forming TM3a helix and in selected other parts of the protein. Mutants were investigated for their expression, stability, and activity and as fluorescent probes of the physical properties along the length of the pore. Most Trp mutants were expressed at levels similar to that of the parent (MscS YFF) and were stable as heptamers in detergent in the presence and absence of urea. Fluorescence data suggest a long hydrophobic region with low accessibility to aqueous solvents, extending from L105/L109 to G90. Steady-state fluorescence anisotropy data are consistent with significant homo-Förster resonance energy transfer between tryptophan residues from different subunits within the narrow pore. The data provide new insights into MscS structure and gating.

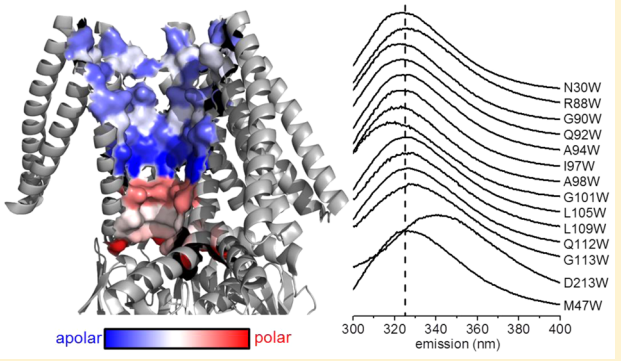

Mechanosensitive channels gate in response to increased tension in the lipid bilayer that arises from lowering of the external osmolarity (hypoosmotic shock).[1−3] A major structural transition takes place to create a large, transient transmembrane pore that is fully hydrated,[4] which allows the transit of small, osmotically active solutes. The pores are usually relatively nonspecific for the solutes, and only molecular volume is a good predictor of which solutes might pass through the channel. The channels have been demonstrated to play a major role in protecting the mechanical integrity of the bacterial cell during hypoosmotic shock[5] and in stabilizing the structure of chloroplasts and yeast endoplasmic reticulum.[6−8] There are two major types of channels, MscL (the channel of large conductance) and MscS (the channel of small conductance),[5,9,10] where the latter is a large family of proteins with many structural variations.[11] Through crystallography, molecular dynamics, biophysical approaches, and molecular genetics, we have come to understand much about the structure of the pore of MscS and the gating process.[4,12−20]

Multiple structures of MscS from different organisms in both nonconducting (closed)[12,21] and conducting (open) configurations[19,21] (a further structure from *Thermoanaerobacter tengcongensis* may also be in the closed state[22]) have been determined. A more condensed state has been proposed on the basis of molecular dynamics.[17] Central to understanding the mechanism is the nature of the closed pore. Thus, the crystal structure shows MscS to be a homoheptamer (and indeed all MscS variants studied to date exhibit masses consistent with a heptamer).[23,24] Each MscS subunit has two transmembrane helices, TM1 and TM2, that form a "sensor" paddle attached to the pore-forming helix, TM3a. All seven subunits contribute a helix to the pore. A pronounced kink after residue Q112 (*Escherichia coli* MscS numbering) leads to an amphipathic helix, TM3b, that has been predicted to lie at the membrane interface with its hydrophobic surface interacting with lipid chains and the hydrophilic face intercalating with the β domain.[12] The pore-forming (TM3a) and pore-sensing domains (TM1 and TM2) are inserted through the lipid bilayer, such that the amino-terminal residues are integrated into the headgroup region of the outer leaflet of the membrane,

Received: March 17, 2015
Revised: June 18, 2015
Published: July 1, 2015

DOI: 10.1021/acs.biochem.5b00294
Biochemistry 2015, 54, 4519−4530

are periplasmic, or form a cap on the pore helices.[25,26] This region is not resolved in any of the crystal structures.[12,19,22] The open pore thus forms a conduit connecting the periplasmic space with the cytoplasm, the latter being achieved through portals formed in the large cytoplasmic vestibule.[12]

In the original crystal structure of the nonconducting MscS, a moderately large "hole" was evident that was, at least partially, sealed by two rings of leucine residues (L105 and L109, *E. coli* MscS numbering).[12] The appearance of the protein suggested the possibility that an open form had been captured. However, measurements of the pore by a variety of methods showed that its diameter was inconsistent with the known conductance of the channel.[27] In parallel, it was proposed, from MD simulations, that the pore was sufficiently hydrophobic to create a vapor lock that would prevent a column of water from forming in the pore and this would block ion conduction.[28,29] Thus, the closed state is nonconducting by virtue of the hydrophobicity of the residues facing into the pore and the tight packing of the TM3a helices. When the open structure was determined,[19] it was clear that the expanded state of the pore was achieved by straightening the TM3a helices and their displacement from the pore axis to create a water-filled pore. The diameter of this pore was shown to be consistent with the known conductance.[19]

Tryptophan substitution mutagenesis has proven to be a valuable tool for the analysis of ion channel structure[30−34] because the unique fluorescence properties of this amino acid allow inferences to be drawn about the environment in which the side chain is located. Tryptophan has the most stringent space requirements of all natural amino acids not only because of its large molecular volume (163 Å^3) but also because of the rigidity of the aromatic side chain. Accommodation of the Trp residue in mutant channels may require an altered conformation that modifies the stability and activity of the channel. However, the susceptibility of Trp fluorescence to lipid-borne and soluble quenchers provides valuable insights into the organization of the protein. For MscS, we have previously shown that Trp can be substituted into the pore for Leu at positions 105 and 109 and the resulting channels assembled in the membrane and retained function in physiological assays, albeit at a lowered level relative to that of the wild type.[15,20] However, when purified, only the L105W variant was stable. This suggested that Trp substitution mutagenesis would provide a useful tool for investigating the pore of MscS, in particular for identifying regions that are sensitive to perturbation. We have previously reported the properties of a Trp-free MscS protein, MscSYFF.[20] The mutant channel possesses protective ability in downshock assays similar to that of the wild type, but in patch clamp assays, it required a tension ∼50% higher than that of the wild type to undergo the transition to the open state.[20] We used this mutant protein for construction of Trp substitutions at each position in pore-lining helix TM3a and at selected positions in TM1 and TM2. In the closed state, TM3a helices pack tightly with a "knobs and grooves" arrangement involving residues 98−101, 102−104, and 106−108.[12,13] The other residues either face into the pore or interact with TM1, TM2, or lipids. The data show that although the structure of MscS may be perturbed by Trp insertion, most of the mutants form stable heptamers that can be purified and reconstituted into lipid bilayers. Modified activity was detected for the mutant channels, both by electrophysiology and by their protective ability during hypoosmotic shock; only a few mutant channels exhibited properties close to those of the wild-type channel in one or more assays. At each position examined, the Trp fluorescence exhibits unique properties with respect to emission maximum and accessibility to water-borne quenching agents and the data are consistent with a very hydrophobic pore.

EXPERIMENTAL PROCEDURES

Materials and Bacterial Strains. Isopropyl β-D-thiogalactoside (IPTG) was obtained from Melford Laboratories (Ipswich, U.K.), *n*-dodecyl β-D-maltopyranoside (DDM) from Affymetrix Anatrace (High Wycombe, U.K.), and 1,2-dioleoyl-*sn*-glycero-3-phosphocholine (DOPC) from Avanti (Alabaster, AL), and all other chemicals were from Sigma-Aldrich (Gillingham, U.K.). *E. coli* strains MJF429 (Frag1 Δ*mscS*, Δ*mscK::Kan*) and MJF612 (Frag1 Δ*mscL::cm*, Δ*mscS*, Δ*mscK::kan*, Δ*ybdG::apr*) were constructed and characterized previously.[5,24]

Molecular Biology and Physiological Assays. The pTrcMscSYFF construct,[20] with mutations W16Y, W240F, and W251F, was used as a template to introduce tryptophan mutations by applying the Stratagene QuikChange protocol. Mutations were confirmed by sequencing on both DNA strands. Survival after osmotic downshock was tested as described previously[14] using transformants of MJF612 grown in Luria-Bertani (LB) medium (10 g/L tryptone, 5 g/L NaCl, and 5 g/L yeast extract) containing 0.5 M NaCl at 37 °C. At an OD_{650} of 0.2, expression of the mutated MscS was induced by addition of 0.3 mM IPTG until the OD_{650} reached 0.3. In parallel, noninduced samples were prepared. The cells were then diluted in LB medium (shock) or diluted in LB medium containing 0.5 M NaCl (control). After incubation for 10 min, serial dilutions were made and spread on LB agar plates with or without 0.5 M NaCl. The plates were incubated overnight at 37 °C, and colonies were counted. It should be noted that the relationship among channel abundance, channel activity, and survival is a complex one for both MscS[13,14,35] and MscL.[36] A more complete discussion of the factors determining the outcome of this assay is provided elsewhere.[35,37] Electrophysiological experiments were performed as described previously.[5,13] Giant protoplasts were generated from MJF429 cells transformed with the relevant constructs after induction with 1 mM IPTG for 15−45 min. Excised, inside-out patches of the protoplasts were analyzed by patch clamp at a membrane potential of −20 mV using the same buffer on both sides of the membrane [5 mM HEPES (pH 7.0), 200 mM KCl, 90 mM $MgCl_2$, and 10 mM $CaCl_2$]. Recordings were performed with an AxoPatch 200B amplifier and pClamp software (Axon) at a sampling rate of 50 kHz and filtration of 5 kHz. The pressure ratios relative to the pressure threshold of MscL (P_L:P_S) are given as a relative indicator of the pressure required to open the mutant forms of MscS as described previously.[38] This analysis could be applied accurately only to channels that exhibited frequent stable openings such that the pressure at which two channels are open simultaneously could be determined.

Purification of MscS Tryptophan Mutants. Purification of the MscS tryptophan mutants followed the protocol established previously.[15,20] Membranes were solubilized by incubation for 1 h at 4 °C in 1.5% DDM containing 50 mM sodium phosphate (pH 7.5), 300 mM NaCl, 10% glycerol, 50 mM imidazole, and 0.2 mM phenylmethanesulfonyl fluoride (PMSF, Sigma). Aggregates were removed by centrifugation at 3000*g* for 10 min and filtration using a 0.2 μm syringe filter. MscS was then bound through its C-terminal His_6 tag to a

DOI: 10.1021/acs.biochem.5b00294
Biochemistry 2015, 54, 4519−4530

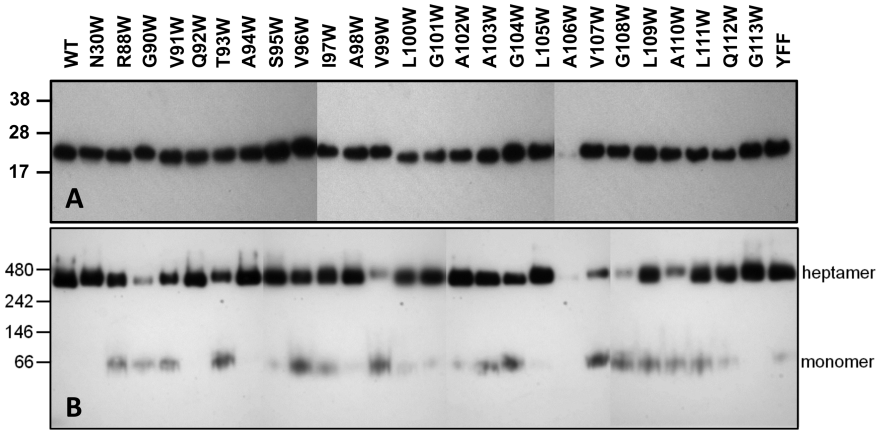

Figure 1. Stability of MscS tryptophan mutants. (A) Western blot of *E. coli* MscS Trp mutants in which 15 μg of membrane protein was loaded on a 4 to 12% sodium dodecyl sulfate−polyacrylamide gel electrophoresis gel and after development Western blotting with antibody specific for the His_6 tag (see Experimental Procedures). (B) Membrane proteins (30 μg) were solubilized in PBS (pH 7.4) containing 1% DDM, 2.8 M urea, and 1 mM EDTA and prepared for BN-PAGE as described in Experimental Procedures. Samples were separated on Novex 4 to 16% Bis-Tris gradient native gels (Invitrogen) and proteins detected by Western blot as described for panel A. The positions of heptameric and monomeric MscS with associated lipids and detergent are indicated.

prepacked 0.5 mL nickel-nitrilotriacetic (Ni-NTA) agarose column (Sigma) and washed with 20 mL of buffer A [50 mM sodium phosphate (pH 7.5) containing 0.05% DDM, 300 mM NaCl, 10% glycerol, and 50 mM imidazole]. After storage overnight at 4 °C, MscS was eluted with elution buffer B (buffer A containing 300 mM imidazole). Peak fractions were separated on a HiPrep Superdex 200 16/600 size exclusion column (GE Healthcare) at a rate of 1 mL min^{-1} using a buffer containing 0.03% DDM, 50 mM sodium phosphate (pH 7.5), and 150 mM NaCl. The ratio of heptamers to monomers was used as a guide to the stability of the mutated channel complex. For fluorescence measurements in bilayers, MscS was reconstituted by dilution into DOPC following a protocol described in detail in ref 39. In short, MscS solubilized in DDM was mixed with DOPC solubilized in sodium cholate (Sigma) at a molar ratio of 1:100 and incubated for 15 min at room temperature. Then the mixture was diluted 30-fold, far below the critical micelle concentration for the detergents, into the measuring buffer containing 40 mM HEPES (pH 7.2), 100 mM KCl, and 1 mM EGTA, and emission spectra were recorded after equilibration for 5 min.

Blue Native Polyacrylamide Gel Electrophoresis (BN-PAGE). MscS constructs were transformed into MJF612 and grown to an OD_{650} of 0.4 in 120 mL of LB medium. MscS was induced by addition of 0.3 mM IPTG and incubation continued for 30 min at 37 °C. Expression of mutant MscS channels in this study did not cause impaired growth upon induction of the transformed *E. coli* strain. Cells were harvested by centrifugation and kept at −80 °C until further use. The cell pellet was suspended in 5 mL of PBS buffer [137 mM NaCl, 2.7 mM KCl, 10 mM Na_2HPO_4, and 2 mM KH_2PO_4 (pH 7.4)] supplemented with 0.2 mM phenylmethanesulfonyl fluoride (PMSF) and lysed by a single passage through a French press at 18000 psi. After centrifugation at 3000*g* for 20 min, 3.2 mL of the supernatant was centrifuged at 100000*g* for 1 h at 4 °C. The membrane pellet was suspended in 125 μL of PBS and frozen in small aliquots at −80 °C until further use. The total protein concentration was determined by the Lowry assay.[40] Membrane suspensions corresponding to 30 μg of protein were solubilized in PBS buffer (pH 7.4) containing 1% DDM, 2.8 M urea, and 1 mM EDTA for 30 min at room temperature. Samples were centrifuged at 14000*g* for 10 min at 4 °C. After addition of native sample buffer and Coomassie G-250 [as per the manufacturer's instructions (Invitrogen)] to the supernatant, samples were loaded onto Novex 4 to 16% Bis-Tris gradient native gels (Invitrogen) and run at 150 V for 2 h. Details of the gel PAGE and the Western blotting followed the protocol of the supplier (Invitrogen).

Fluorescence Spectroscopy. Fluorescence spectroscopy was performed as described in detail previously[15,20] using an FLS920 fluorescence spectrometer from Edinburgh Instruments (Livingston, U.K.). For steady-state emission spectra, tryptophan was excited at 295 nm with a slit width of 2 nm and the emission was recorded between 300 and 420 nm with a slit width of 2 nm. Reconstituted samples were measured with slit widths of 3 and 7 nm. A 0.2 mL micro cuvette with 10 mm excitation and 4 mm emission path lengths was used (Hellma). The excitation polarizer was set to 90° and the emission polarizer to 0°.[41] The spectrum was fitted to a skewed Gaussian after correction with a buffer spectrum:

$$I = I_{max}\ \exp((-\ln 2)\{\ln[1 + 2b(\lambda - \lambda_{max})/\omega_\lambda]/b\}^2) + a \quad (1)$$

where I is the wavelength-dependent fluorescence intensity, I_{max} the maximal intensity, b a skewing factor, λ the emission wavelength, λ_{max} the wavelength of the peak, and ω_λ the width of the peak at half-maximal intensity. Quenching by acrylamide in the concentration range of 0−0.2 M was quantified using the Stern−Volmer equation:

$$I_0/I = 1 + K_{SV}[Q] \quad (2)$$

where I_0 and I are the fluorescence intensities in the absence and presence, respectively, of a quencher at concentration [Q]. K_{SV} is the Stern−Volmer constant, which quantifies the dynamic quenching for a given position.

Steady-state anisotropy r was measured at an excitation wavelength of 295 nm and in an emission range of 340−360 nm both with a slit width of 2 nm. The anisotropy was determined according to eq 3 considering the instrumental G factor = I_{hv}/I_{hh}:

$$r = (I_{vv} - GI_{vh})/(I_{vv} + 2GI_{vh}) \quad (3)$$

DOI: 10.1021/acs.biochem.5b00294
Biochemistry 2015, 54, 4519−4530

The first and second subscripts indicate the position of the excitation and emission polarizers (v for vertical and h for horizontal), respectively.

RESULTS

Expression and Stability of the MscS Trp-Substituted Channels. With the single exception of A106W, expression and integration into the membrane were observed (as detected by Western blot for the His tag) for all the mutated MscS channels (Figure 1A). Blue native (BN) PAGE analysis in combination with Western blots is a convenient tool for assessing the oligomeric state of MscS without the requirement for full purification.[42] Preliminary work established that detergent solubilization alone did not destabilize the protein. Thus, the oligomeric state was assessed by incubation under mildly destabilizing conditions (2.8 M urea and 1 mM EDTA). Under these conditions, wild-type (WT) MscS, YFF, and 14 of 25 mutant proteins were essentially heptameric (Figure 1B). Only seven of the mutant channels exhibited significant levels of monomer after extraction in the presence of urea and EDTA (G90W, T93W, V96W, V99W, V107W, G108W, and A110W). Five other mutants exhibited some breakdown of the heptamer in the presence of urea. Thus, the majority of the Trp mutants display remarkable stability. This observation was supported by analysis of a limited series of proteins by size exclusion chromatography utilizing just those channels that were subsequently studied by fluorescence (Figure 2). For fluorescence analysis, it is critical that the properties of the Trp residues reflect the heptameric state rather than any monomers that might arise after extraction from the membrane. Five of 14 mutants exhibited significant levels of monomer in the purified protein. Thus, WT protein eluted from the size exclusion column predominantly as a single symmetrical peak (Figure 2). We have previously reported that L109W is unstable and this protein was used to validate the assay (Figure 2).[15] Unstable proteins, particularly R88W, I97W, A98W, and G101W, exhibited increased amounts of the monomer and decreased amounts of the heptamer. Some mutant proteins exhibited a shift in the elution volume (e.g., N30W and Q112W), and the elution profile for others exhibited a small peak on the leading shoulder for the heptameric protein consistent with formation of higher-order oligomers (A94W, A98W, and G113W). G90W, which was expressed well (Figure 1A) but very unstable in the presence of DDM and urea (Figure 1B), could not be purified in significant quantities (Figure 2). The small amount of pure protein obtained was distributed between the heptamer and monomer, again suggesting extreme instability caused by the Gly to Trp change at this position.

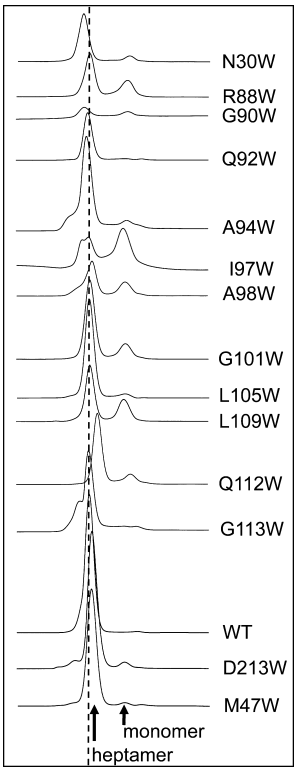

Figure 2. Size exclusion chromatographs of selected MscS tryptophan mutants. Heptameric and monomeric MscS were separated on a HiPrep Superdex 200 10/600 GL size exclusion column as described in Experimental Procedures. A vertical dashed line indicates the heptamer position for WT MscS.

Physiological Characterization of the Mutant Channels. By three criteria [expression, stability after purification, and BN-PAGE after DDM/urea extraction (Figures 1A,B and 2)], the majority of the Trp mutants are stable proteins suitable for analysis. Previous studies have established that the expression of MscS at the basal level driven by the Trc promoter gives moderate protection to a strain deleted for MscS, MscK, MscG (YbdG), and MscL (MJF612) and that overexpression by induction with IPTG leads to complete protection.[14] The survival assay works best as a predictor of loss of either expression or function in mutated channel proteins.[13,35−37] MscS channels that are poorly expressed or have impaired function (or both) provide only limited protection, and this is most easily seen when the channel expression has not been induced.[37,43,44] The majority of the Trp mutant channels failed to afford protection when expressed at this basal level, which is 8−10-fold below the expression level normally seen for the fully induced WT protein (Figure S1 of the Supporting Information and Figure 3A), but were protective after induction with IPTG (Figure 3B). The exception was T93W, which protected even when expressed at a basal level (Figure 3A). Several mutant channels (R88W, G90W, V91W, V96W, G108W, A110W, and Q112W) exhibited complete loss of protective ability despite being present in the cell membrane. Similar observations have been made for some mutations affecting the MscL channel.[45]

The electrical signature of the Trp mutant MscS channels was investigated using MscL as a reference point for the activation threshold for the mutant channels.[38] The electrical signatures of the mutants were position-specific and could be broken down into four principal groups with respect to the stability of the openings, the conductance, and the pressure sensitivity. Seven mutants (M47W, T93W, S95W, I97W, G101W, G104W, and L111W) exhibited essentially normal channel openings, but there were small differences in the P_L:P_S ratio (Table 1 and Figure 4). However, the majority of the mutants were found to exhibit either reduced conductance or no conductance at all, and many also failed to form fully open states, which precluded detailed analysis of their pressure dependence (Table 1 and Figure S2 of the Supporting Information). Insertion of Trp at positions V91, Q92, and A94, which all map to the neck of the pore, generated channels that were expressed (Figure 1A), exhibited some protection

DOI: 10.1021/acs.biochem.5b00294
Biochemistry 2015, 54, 4519−4530

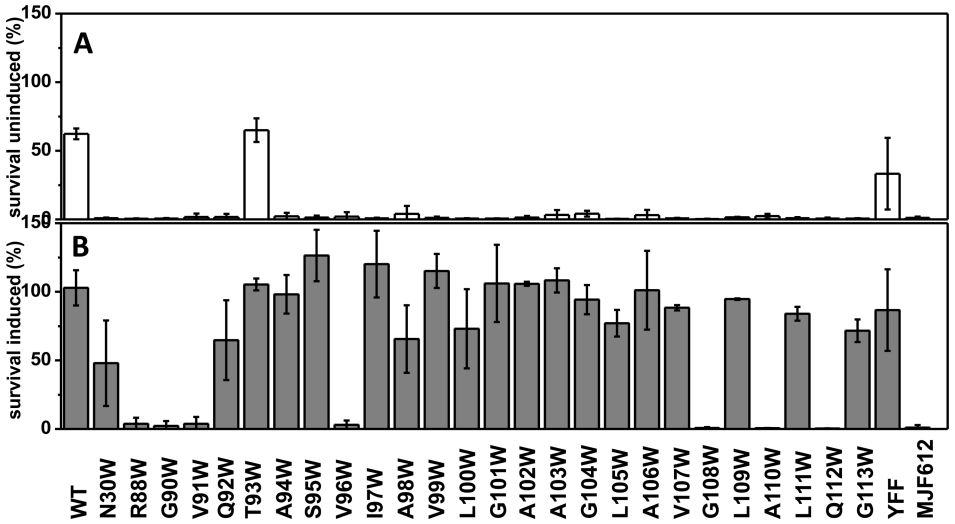

Figure 3. Protection against hypoosmotic shock. Transformants of MJF612 (lacking MscL, MscS, MscK, and YbdG) expressing individual MscS Trp mutants were assessed for survival after a 0.5 M NaCl hypoosmotic shock. Mutants were either expressed as a result of the escape promoter activity of the pTrc promoter (A)[14] or induced during growth (B; 0.3 mM IPTG for 30 min) immediately prior to downshock (see Experimental Procedures). Data are means and the standard deviation of three independent cultures.

against downshock (Figure 3B), but failed to exhibit currents despite the observation of MscL channels in the patches (Table 1). Three mutants (V96W, A103W, and V107W) opened to the full extent, but the open state was unstable (Table 1).

A unique property was observed with V99W. At low pressures (P_L:P_S = 1.8−2.4), its conductance was similar to that of MscSYFF [∼1.1 ± 0.01 nS (n = 5)]; however, the channel flickered, and transitions to subconducting states were frequently observed (Figure 5A), indicating that the open state was unstable. However, if the pressure on the patch was increased (P_L:P_S = 1.17−1.49), stable openings that were ∼50% larger than that of the WT [1.64 ± 0.02 nS (n = 5) (Figure 5D)] were observed, and these exhibited a stability similar to that of MscS (Figure 5A). In the closed crystal structure [Protein Data Bank (PDB) entry 2OAU], V99 is exposed in the crevice between TM1/TM2 and TM3a, which could accommodate the increased volume of Trp (∼50% increase relative to that of Val). In the open crystal structure (2VV5), it is observed that the movement of TM3a outward from the pore axis (to create the open pore) juxtaposes Val99 with Phe80, which could generate a potential conflict between V99W and F80 causing an unstable open state, but at higher pressures, the two residues might form a $\pi-\pi$ stack that stabilizes the more conducting stable state (Figure 5B,C). Thus, we created a V99W/F80A double mutant to introduce a compensating drop in amino acid side-chain volume at position 80 and to remove the potential for $\pi-\pi$ stacking. The resulting channel exhibited electrophysiological properties close to those of MscSYFF (P_L:P_S = 1.54 ± 0.06; γ ∼ 1.1 nS; n = 3) (Figure 5A, bottom panel).

Polarity and Water Accessibility Detected by Fluorescence Spectroscopy. Tryptophan is a sensitive fluorophore that reports the physical properties of its environment.[46] We investigated the fluorescence of detergent-solubilized MscS channels with Trp at a number of positions between R88 and G113. Positions in TM3a in which the native residue side chain is oriented toward the pore were chosen, and in addition, three mutants were investigated in the periplasmically exposed region of the closed crystal structure of the channel (N30W, R88W, and G90W). Two further mutants were created as reference points: D213W is located on the surface of the cytosolic domain and represents a residue completely exposed to the bulk water phase, and M47W is in the middle of TM1. Size exclusion chromatography revealed that several mutant forms are less stable than WT MscS as discussed above. These were in particular R88W, G90W, I97W, and A98W. If the protein were a mix of heptamers and monomers in detergent, then this would compromise the analysis of fluorescence because the data would represent the mix of proteins in multiple different states. Anisotropy measurements using separate pools of monomers and heptamers (see below) suggest that the complex stays intact during measurement.

The peak position for each of the Trp residues was blue-shifted relative to both the native Trp residues in the soluble domain (λ_{max} = 334 nm for W240 in a mutant in which the proximal Trp residue W251 had been mutated to Phe[20]) and the surface-exposed Trp mutant, D213W (Table 2). The emission maxima clustered together for most of the mutants with the exceptions of A103W, G101W, G113W, and D213W (Table 2 and Figure 6). The most blue-shifted, representing the most hydrophobic environment, was A103W (λ_{max} = 310.5 ± 0.4 nm), and this residue was least accessible to quenching by acrylamide (Table 2 and Figure 6). This residue and T93W were the only residues we studied by fluorescence in TM3a that are outward-facing (i.e., oriented away from the pore) in the crystal structures. Overall, a correlation (R = 0.97) was seen between λ_{max} and K_{SV}, which reports accessibility to the aqueous quenching agent, acrylamide.[47] It is difficult to predict the precise positioning of the Trp side chain in the mutants, but the λ_{max} and K_{SV} values (Table 2) are consistent with a hydrophobic environment that is relatively inaccessible to aqueous quenching agents (Figure 7), though in principle stationary water could also cause a blue-shift of λ_{max} depending on the position of the water dipole relative to the fluorophore.[48] A surprising observation was that Trp residues located at positions L105 and L109 reported significantly polar environments and were moderately accessible to acrylamide (Table 2 and Figure 7). Toward the cytosolic vestibule, the acrylamide accessibility is increased at G113W, which is consistent with the higher λ_{max} [329.7 ± 1.3 nm (Table 2)].

DOI: 10.1021/acs.biochem.5b00294
Biochemistry 2015, 54, 4519−4530

Table 1. Channel Characteristics Determined by Patch-Clamp Electrophysiology[a]

character	mutant	P_L:P_S	n value
WT[b]	YFF	1.36 ± 0.06	6
	M47W	1.30 ± 0.08	4
	T93W	1.26 ± 0.05	6
	S95W	1.02 ± 0.04	7
	I97W	1.33 ± 0.08	6
	G101W	1.03 ± 0.08	6
	G104W	1.33 ± 0.13	3
	L111W	1.19 ± 0.08	3
no activity[c]	V91W		6
	Q92W		5
	A94W		8
short dwell	V96W	nd[f]	4
	A103W	1.31 ± 0.18	6
	V107W	1.28 ± 0.24	3
variable[d]	N30W	nd[f]	4
	R88W[e]	1.04 ± 0.03; nd	5
	G90W	nd[f]	4
	A98W	nd[f]	4
	L100W	nd[f]	5
	A102W	1.04 ± 0.04	4
	L105W	nd[f]	7
	A106W	nd[f]	3
	G108W	nd[f]	4
	L109W	nd[f]	3
	A110W	nd[f]	4
	Q112W	nd[f]	4
	G113W	1.66 ± 0.19	5
high conductance	V99W[e]	1.8−2.4; 1.17−1.49	5

[a]Channel activity was measured as described in Experimental Procedures using cells expressing unique MscS variants that had been induced with IPTG. Whereas the channels most like WT (YFF, M47W, and T93W) were induced for 15 min with 1 mM IPTG, the other channels required an induction period of up to 45 min for channels to be detected in the patches. The voltage was set to −20 mV. [b]WT indicates that the channel gives rise to a stable open state typical of MscS with a conductance ∼1.1 nS. [c]Only MscL openings were detected in patches with no evidence of MscS channel activity (n refers to number of patches in which MscL activity was detected but no MscS). [d]Flickery channels failed to reach a stable conductance equivalent to that of WT MscS, and multiple rapid openings and closures were observed in response to increased pressure on the patch. [e]Two distinct conductance states were observed, with the second conductance state arising after the application of further pressure. [f]Insufficiently stable channel openings were observed that correspond to the full conductance of MscS, and therefore, P_L:P_S ratios could not be obtained.

Our data agree well with bulk water accessibilities determined by spin-labeling and electron paramagnetic resonance (EPR) spectroscopy in the presence of the relaxation agent NiEDDA.[26,49] In particular, these data also show the low accessibility of the funnel region (V89−A94).

Steady-State Anisotropy as a Tool for Obtaining Pore Shape Information. The steady-state anisotropy is sensitive to the mobility of the fluorophore on the time scale of its fluorescence lifetime, which is in the nanosecond range for tryptophan. Therefore, tryptophan anisotropy is typically sensitive to side-chain rotation, but the overall tumbling of MscS is too slow. Anisotropy is influenced by the mobility of the fluorophore, but also by homo-Förster resonance energy transfer (homo-FRET),[50] and reflects the proximity of two Trp residues. Fluorescence anisotropy may also be sensitive to dissociation of the complex when homo-FRET between Trp residues from different subunits is a significant factor[51,52] (see below). Comparing the dissociated fraction from the SEC with the heptameric fraction for I97W showed anisotropy (r = 0.180 ± 0.007 and r = 0.143 ± 0.004 for monomer and heptamer, respectively) and similarly for A98W (r = 0.165 ± 0.008 and r = 0.122 ± 0.01, respectively). These differences were maintained during measurements with DDM-solubilized proteins, indicating that even for these more fragile mutants the heptameric complex stayed intact for the fluorescence experiments. Given that these were the least stable proteins, it is reasonable to conclude that the fluorescence properties for all the mutants principally reflect the heptameric state, but for the unstable mutants, the results should be treated with more caution.

Steady-state fluorescence anisotropy data mirror the shape of the pore in MscS. Trp residues in TM1 (N30W and M47W) exhibited high anisotropy, reflecting their relatively constrained position (Table 2). The M47W and N30W residues lie on the mobile TM1−TM2 helix pair paddle and would not be expected to exhibit significant Trp−Trp interaction. However, in the highly packed pore domain, a low mobility and therefore a high anisotropy would be expected. The lowest anisotropy was observed at the narrowest part of the channel between A98 and Q112, but A103W was atypical in exhibiting a high anisotropy consistent with an outward orientation of this mutant and therefore low homo-FRET. At the periplasmic funnel (R88−Q92) and at the cytosolic entrance to the vestibule (G113), higher anisotropies were found, consistent with larger Trp−Trp distances and therefore lower homo-FRET than in the narrow pore (Table 2 and Figure 7B). In the heptamer, the Trp residues at the two seal rings (L105W and L109W) from the different subunits must come close to each other, which would allow homo-FRET. The Förster distance for Trp homo transfer ($R_0 \approx 10$ Å) is in the range of the closed pore diameter.[53,54] Measurements on the dissociated complex from L109W confirm that the data are dominated by homo-FRET because the dissociated complex of L109W has an anisotropy r of 0.172 ± 0.007 versus a value of 0.117 ± 0.002 within the complex. A similar effect is seen for I97W, as reported above; these residues are expected to be separated by ∼9 Å (measured C_β−C_β distance) in the range of residue separation in the closed pore. The cytosolic domain control residue D213W exhibited a low anisotropy, suggesting a high side-chain mobility that is consistent with the expected red-shift of the emission maximum (Table 2). Homo-FRET is unlikely to be a factor here because of the large distances between the Trp residues (∼37 Å).

The anisotropy data were fitted using the C_β−C_β distances of the same residue in neighboring subunits obtained from the closed and open structures (PDB entries 2oau and 2vv5, respectively) assuming a FRET mechanism. Previous analysis suggests that the channel is in the open state when it is solubilized in DDM.[55,56] The data could be fitted to C_β−C_β distances from either the open or the closed state, but the fit was better for the latter (Figure S3 of the Supporting Information). Data from the two extremities (Q92W and T93W, and L109W and Q112W) of the pore appeared to cause a poorer fit for the open state. However, elimination of these data either separately or together improved the fit but not to give a result equivalent to that for the fit for the closed state (Figure S3 of the Supporting Information). These differences may reflect the impact of Trp substitution on the balance

DOI: 10.1021/acs.biochem.5b00294
Biochemistry 2015, 54, 4519−4530

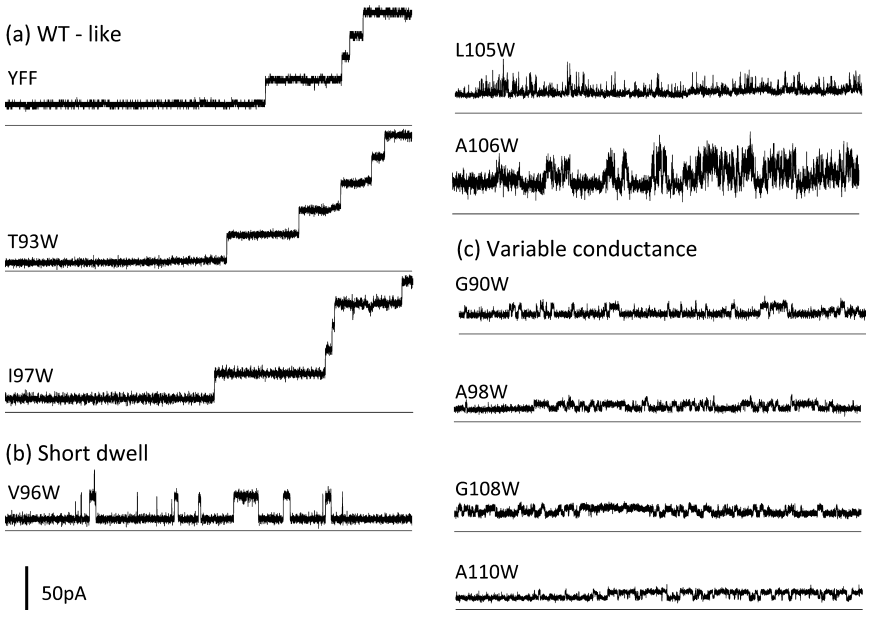

Figure 4. Representative electrophysiology traces for selected Trp mutants. When assayed by patch clamp electrophysiology on isolated patches, Trp mutants were found to have four different types of behavior. Three are shown here: (a) WT-like, (b) short dwell, and (c) variable conductance (the fourth type of behavior was the lack of channel activity in the patch other than MscL, and these data are not shown). Additional data are shown in Figure S1 of the Supporting Information.

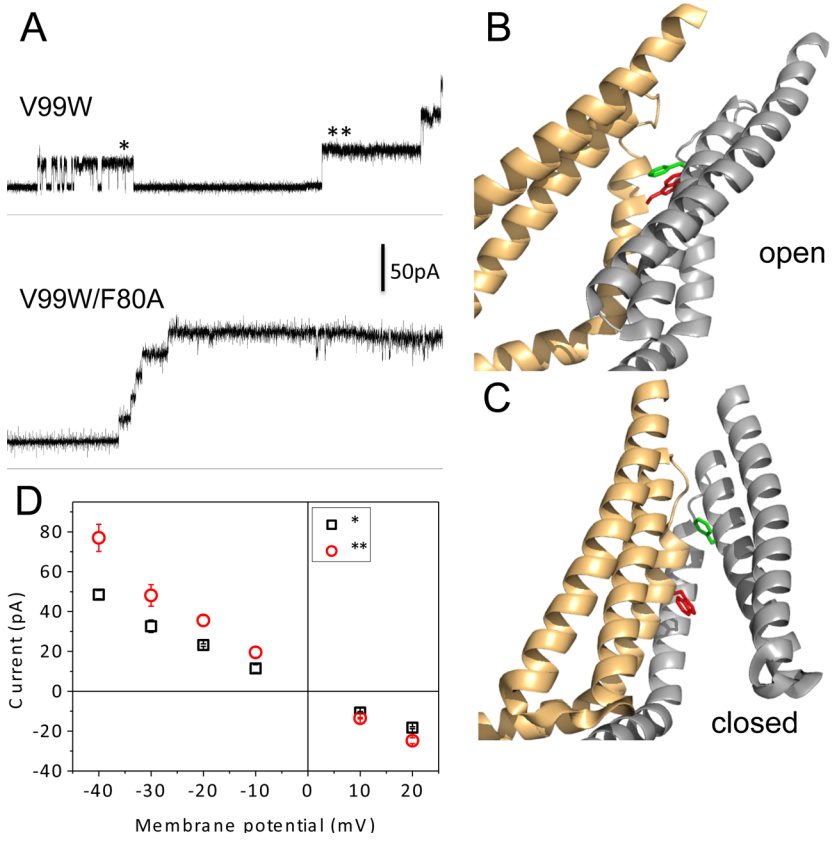

Figure 5. V99W generates two distinct open states. (A) Opening of V99W at "normal pressures" showed short dwell openings with WT-like conductance (one asterisk, ~24 pA), but as the pressure was increased, channel openings (two asterisks) were associated with higher conductance and stable openings were observed (~34 pA, ~1.7 nS) (top). In the double mutant, V99W/F80A, only stable conductances of WT magnitude (~23 pA, ~1.2 nS) were observed (bottom). The high conductance may be explained by a $\pi-\pi$ interaction between V99W and F80 on adjacent subunits (i.e., V99W:a with F80A:b) in the open state (B; PDB entry 2VV5), whereas the residues are well-separated in the closed state (C; PDB entry 2OAU) (V99W is colored red and F80 green). Only two subunits are shown for the sake of clarity. Models and figures were produced with PyMol. (D) Current-voltage plot for V99W at low (*; see panel 5A) (Black open squares) and high (**; see panel 5A) (red open circles) pressure, as described in text.

DOI: 10.1021/acs.biochem.5b00294
Biochemistry 2015, 54, 4519−4530

Table 2. Fluorescence Properties of Tryptophan Mutants[a]

mutant	λ_{max} (nm)	K_{SV} (M^{-1})	anisotropy	C_β–C_β distance (Å)	b value
N30W	323.1 ± 0.5	2.9 ± 0.6	0.161 ± 0.004	14.5 ± 1.3	207 ± 1
R88W	325.1 ± 0.9	1.2 ± 0.2	0.184 ± 0.005	14.0 ± 1.0	170 ± 9
G90W	322.8 ± 0.5	1.2 ± 0.4	0.162 ± 0.010	12.1 ± 1.0	166 ± 5
Q92W	323.2 ± 1.2	2.6 ± 0.3	0.172 ± 0.007	9.8 ± 0.3	160 ± 2
T93W	321.4 ± 0.1	1.8 ± 0.1	0.181 ± 0.002	11.1 ± 0.3	149 ± 4
A94W	322.5 ± 2.7	2.4 ± 0.1	0.136 ± 0.010	8.0 ± 0.2	143 ± 3
I97W	322.7 ± 0.7	1.7 ± 0.3	0.143 ± 0.004	8.4 ± 0.1	118 ± 4
A98W	321.7 ± 1.5	2.3 ± 0.1	0.122 ± 0.010	7.8 ± 0.4	114 ± 4
G101W	315.2 ± 3.3	0.9 ± 0.6	0.132 ± 0.008	7.3 ± 0.1	104 ± 5
A103W	310.5 ± 0.4	0.3 ± 0.1	0.167 ± 0.012	11.9 ± 0.3	105 ± 5
L105W[b]	327.7 ± 0.6	2.5 ± 0.3	0.135 ± 0.012	6.4 ± 0.1	100 ± 5
L109W	325.9 ± 1.4	1.7 ± 0.6	0.117 ± 0.002	7.2 ± 0.2	97 ± 8
Q112W	326.6 ± 0.3	1.8 ± 0.2	0.122 ± 0.009	8.8 ± 0.5	108 ± 6
G113W	329.7 ± 1.3	3.6 ± 0.4	0.185 ± 0.003	10.7 ± 0.3	99 ± 5
controls					
M47W	326.7 ± 0.1	1.9 ± 0.1	0.177 ± 0.004	27.7 ± 2.3	224 ± 2
D213W	340.6 ± 0.5	7.7 ± 0.1	0.123 ± 0.001	36.9 ± 0.2	104 ± 6

[a]Positions of the emission peak λ_{max}, Stern–Volmer constant K_{SV} for quenching experiments with acrylamide, and steady-state anisotropy are shown. Mean values and standard deviations are given. [b]Data for L105W were previously reported in ref 15. Distances of C_β atoms from neighboring subunits were obtained from the closed crystal structure (PDB entry 2OAU), and means and standard deviations are given for the distances in the asymmetric complex. For glycine residues, the corresponding modeled H atoms were taken using PyMol. b values for C_β atoms from the closed structure are given or, in the case of glycines, for C_α atoms (PDB entry 2OAU).

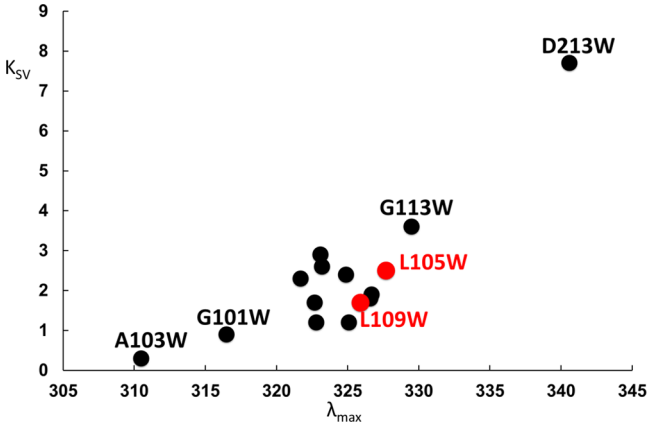

Figure 6. Relationship between the λ_{max} for Trp fluorescence and K_{SV}, the Stern–Volmer constant. Fluorescence spectroscopy was performed as described previously[15,20] on DDM-solubilized proteins. For λ_{max} measurement, Trp residues were excited at 295 nm with a 2 nm slit width and emission was recorded between 300 and 420 nm with a slit width of 2 nm. A 0.2 mL microcuvette was used with 10 mm excitation and 4 mm emission path lengths. For K_{SV}, quenching by acrylamide in the concentration range of 0–0.2 M was quantified (see Experimental Procedures). The data for L105W and L109W are colored red.

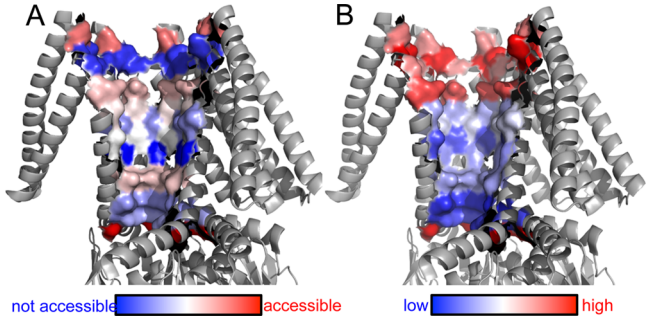

Figure 7. Water accessibility and fluorescence anisotropy of the MscS pore surface. (A) Accessibility to the bulk water phase was detected by quenching of the tryptophan fluorescence by acrylamide. Strong quenching is colored red and weak quenching blue. (B) Steady-state fluorescence anisotropy is shown where blue indicates low values and red high values. If the mobility is comparable for all mutants, the pore shape is reflected by anisotropy because of the changing efficiency of homo-Förster resonance energy transfer. For the sake of clarity, only five of the seven subunits are shown. The figures were generated with PyMol on the basis of the closed crystal structure (PDB entry 2OAU).

between open and closed states in DDM, which has previously been observed for MTSET-modified Cys mutants of MscS.[55] However, it must also be noted that the C_β–C_β distances are not accurate representations for the fluorophore separations; rather, they are just estimates and also make no allowance for structural changes imposed by packing the Trp side chain. Further, one cannot accurately predict the angles between the fluorophores, which is a major factor for FRET.[46]

Reconstitution of Trp Mutants into DOPC Bilayers. Reconstitution of MscS into DOPC liposomes has frequently been used to study the electrophysiological properties of the channel.[9,57] Similarly, a method has been developed for purification and reconstitution of MscL Trp mutants into membrane fragments to investigate lipid–protein interactions.[58–60] We applied the latter method to purified mutants of MscS and measured the emission spectra of the Trp residues. Six positions were investigated (Figure 8); four were found not to exhibit significant changes in their emission maxima upon being reconstituted (T93W, A103W, L105W, and G113W), whereas A94W and G101W were red-shifted. The latter changes are consistent with significant structural changes upon reconstitution and with an environment that is more accessible to water. Thus, in the Trp mutants, these residues may be exposed either in the pore (both residues) or in the periplasmic funnel (A94W). BN-PAGE after the fluorescence measurements showed that MscS retained the heptameric state during reconstitution (Figure S4 of the Supporting Information).

DOI: 10.1021/acs.biochem.5b00294
Biochemistry 2015, 54, 4519–4530

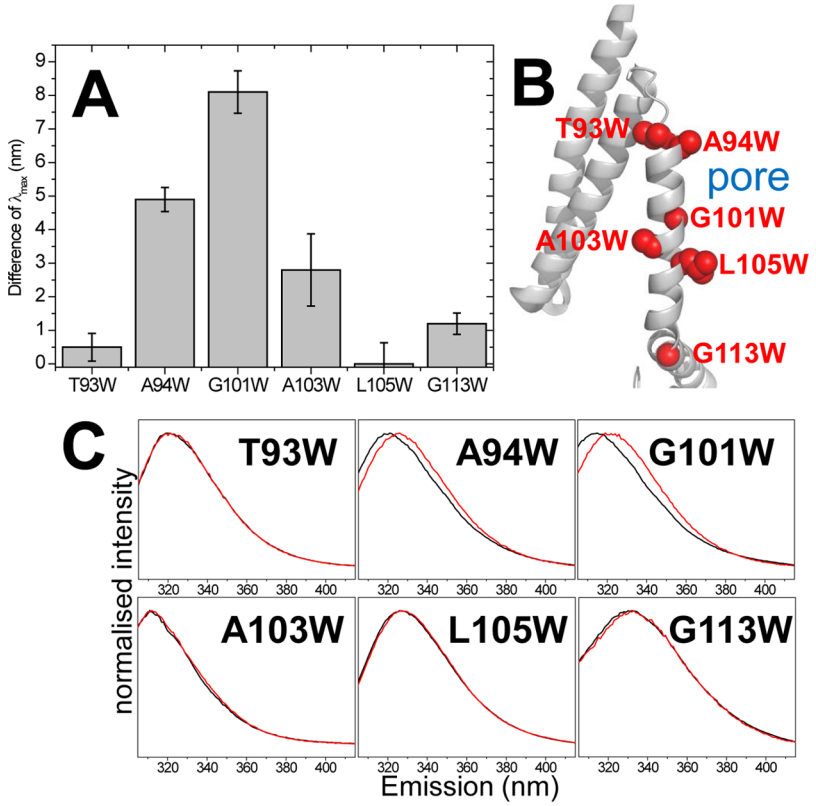

Figure 8. Emission maxima of selected MscS mutants in DDM and reconstituted into membrane bilayers. Six Trp mutants were purified and reconstituted into DOPC bilayers and the emission spectra recorded as described in Experimental Procedures. (A) The red-shift of the emission maxima can be seen in particular for residues in the hydrophobic section of the pore. (B) The positions of the residues are shown on the closed structure 2OAU. (C) Emission spectra of DDM-solubilized samples (black) and samples reconstituted into DOPC (red) are compared.

DISCUSSION

The very special properties of tryptophan make it among the more informative amino acid replacements that can be made.[15,32,34,47,61,62] Care must be taken with membrane proteins because of the known role of this amino acid in controlling topology by anchoring the periphery of transmembrane helices to the phospholipid headgroups of the bilayer.[63,64] Mechanosensitive channels are notable in lacking these "anchorages" but do contain Trp at other positions.[44] We have previously established that only a mild impairment of function results from replacement of the three native Trp residues in *E. coli* MscS with Tyr or Phe.[20] The sensitivity to gating tension is significantly affected by W16, which lies on the periplasmic side of the membrane and exhibits properties typical of a Trp in a hydrophobic environment. A mutation to Tyr (W16Y) mildly impairs the gating sensitivity compared to that of the wild type.[20] Thus, a Trp-free mutant (MscS YFF) is both stable and active, and it was from this platform that the current study was launched.

An important caveat attends Trp scanning mutagenesis. Insertion of the bulky Trp residue may perturb the packing of the protein, and its accommodation may require either subtle or severe adjustments of the structure depending on the position of the affected residue. Indeed, the observed conductance values for I97W and G101W could be interpreted to conflict with the open crystal structure (PDB entry 2VV5) but might be accommodated by other models[25] for the open state in which the pore is predicted to be wider than seen in the open crystal structures.[4,19,25] However, such an interpretation would require an intimate knowledge of the rotamer configuration in the Trp mutants. Thus, the crystal structure is a reasonable guide only in the sense that one can analyze the current packing for each native residue and understand what intrinsic limitations may exist for the Trp substitution. This is graphically illustrated for the least stable mutant G90W, which though expressed and integrated into the membrane, is nonfunctional in physiological assays, forms channels with diminished conductance and stability, and readily dissociates in the presence of urea and detergent (Figure 1B and Table 1). Analysis of the MscS structure (either open, 2vv5, or closed, 2oau) indicates that there is potentially room for the Trp side chain projecting into the periplasmic funnel, which could explain how the protein can be expressed and be inserted into the membrane. Some rearrangement would be required because position 90 is surrounded by eight residues within van der Waals distances (residues 86−89A, 91A, 92A, 87G, and 88G, where A and G refer to the subunits). Moreover, G90 forms the loop in which the torsion angles are $\Phi = +75°$ and $\Psi = -3°$ in the closed structure and $\Phi = +55°$ and $\Psi = +50°$ in the open structure. In the Ramachandran plot,[65] only G fits these parameters and there must be conformational change to allow the G90W mutation. This protein is then unstable once the lipid bilayer is replaced by a DDM micelle. In contrast to this, T93W forms an essentially WT channel; it is notable that Trp is found at the position equivalent to T93 in the *E. coli* YjeP and MscK proteins. Equally notable is the fact that insertion of Trp at positions adjacent to T93 (i.e., Q92W and A94W) leads to channels that could not be detected by electrophysiology despite good expression, a channel stable to urea and DDM and protective function in physiological assays (Table 1).

DOI: 10.1021/acs.biochem.5b00294
Biochemistry 2015, 54, 4519−4530

Channel activity was close to that of the wild type for only a few of the mutants. For the others, the openings were of short duration and exhibited reduced conductance. Where it could be measured accurately, which relies on simultaneous openings of two channels,[38] the gating tension measured in the P_L:P_S ratio was decreased [ratios close to 1 (Table 1)]. For some of the positions, such as the packing residues (G101, G104, G108, A98, A102, and A106), it was a surprise that these mutant channels gated. From the closed structure, it is clear that the Gly and Ala residues on the TM3a pore helix are in the proximity of each other.[13,66] Previously, we have shown that increasing the bulk of these residues decreases the propensity to make the transition to the open state. Thus, given the importance of residue size at these positions,[13] it was surprising to be able to observe gating but no surprise that high pressure was required on the patch to effect the structural transition (Table 1). Among the modified properties, V99, N30, and R88 were most readily addressed from the crystal structures of MscS. The residues in TM1 (N30) and TM2 (R88) are adjacent in the crystal structure (Figure S5 of the Supporting Information) and are predicted to form a H-bond (see the OCA database for 2oau).[67] Such proximity indicates a potential packing change when Trp is substituted at either position. Correspondingly, the properties of the two mutant channels are extremely similar (Figure 4). Novel residue−residue interactions consequent upon introduction of a Trp side chain may explain the observations for V99W. Two conductance states were observed: short-lived openings (~1.1 nS) at pressures associated with gain-of-function (GOF) mutants (P_L:P_S = 1.8−2.4) and larger stable openings (1.64 nS), in the normal range of gating pressure (Figure 5). In the closed state, the V99W mutation can be accommodated between TM3a and TM1/TM2, possibly with TM1/TM2 being moved in the direction found in the open state, which would be consistent with the GOF properties in electrophysiological assays. A further increase in pressure would juxtapose F80 on TM2 of the adjacent subunit with V99W on TM3a, such that the two residues could stack and this might stabilize the channel in a "supra-open state" with the observed higher conductance. Correspondingly, the double mutant, V99W/F80A, exhibited conductance close to that of the wild type, consistent with the open state now being accommodated by the reduced molecular volume at residue F80A.

Keeping MscS closed when the bilayer tension is low is essential for preserving chemical and electrical gradients across the cytoplasmic membrane and is as important as allowing specific passage of solutes after gating.[14,68,69] It has been proposed that the solution to this problem for MscS is the creation of a vapor lock by two rings of leucine, L105 and L109.[25,28,29] Genetic data have already established the importance of this seal, because substitution of small residues, as in L105A and L109A, leads to channels that gate more readily than the wild type.[14] In addition to the narrowing of the pore at this constriction, the hydrophobicity of the walls is a second important factor to make an exclusion of water energetically favorable[29] and thus generate a nonconducting state. Our data indicate that residues beyond the hydrophobic seal at L105 and L109 toward the periplasmic side may play an important role in the hydrophobic sealing of the closed pore, supporting a model with a vapor lock that extends beyond the seal residues.[28] Fluorescence emission maxima for Trp at positions that line the pore indicate particularly low polarity and low accessibility to water-soluble quenchers in this region. It was surprising to find a red-shift of the emission peaks upon reconstitution of MscS into lipid bilayers in this region tested on A94W and G101W. These data illustrate the problems that arise when trying to reconcile mutant data with crystal structures and models that are essentially derived from the WT protein. It would be expected from the crystal structures and the models that A94 and G101 should become more buried in the closed structure. One expects the closed structure for the protein reconstituted into a lipid bilayer. However, the A94W and G101W Trp residues report a more hydrophilic location when the samples are transferred from the detergent-solubilized state to being integrated in the membrane bilayer after reconstitution. The relatively high polarities and accessibility to the acrylamide quencher for the Trp mutants at L105 and L109 may be caused by the mixed character of this amino acid, with the capacity for H-bonding influencing the water structure in the mutants. However, spin-labeling and EPR spectroscopy at these positions produced similar results.[26] A low accessibility to the bulk water phase was observed for an extended region from the hydrophobic seal toward the periplasm; residues 98−104 become more accessible during opening,[19,49] and L105 shows a slightly higher accessibility.

CONCLUSIONS

Tryptophan scanning mutagenesis demonstrated that steric stringency is important in two regions of the TM domain: at the hinge between TM2 and TM3 and in the seal region from A106 to A110. Fluorescence spectroscopy indicates that a hydrophobic region between seal residues L105 and I97 may provide an extended vapor lock. Furthermore, it was found that the periplasmic funnel is surprisingly hydrophobic despite widening toward the water bulk phase. The N-terminal periplasmic domain not resolved in crystal structures could cap the funnel and explain these properties. Finally, fluorescence anisotropy was demonstrated to be a potent tool in the structural biology of mechanosensitive channels.

ASSOCIATED CONTENT

Supporting Information

Detection levels of MscS by Western blotting, electrophysiological characterization of selected mutants, fitting of the distance dependence of anisotropy data, BN-PAGE analysis of reconstituted Trp mutants, and an image of the interaction between R88 and N30 MscS. The Supporting Information is available free of charge on the ACS Publications website at DOI: 10.1021/acs.biochem.5b00294.

AUTHOR INFORMATION

Corresponding Author

*E-mail: i.r.booth@abdn.ac.uk.

Present Address

§S.S.: School of Biosciences, University of Birmingham, Edgbaston, Birmingham B15 2TT, U.K.

Author Contributions

T.R. and A.R. contributed equally to this research.

Funding

This work was supported by a Wellcome Trust Programme grant [092552/A/10/Z awarded to I.R.B., S.M., J. H. Naismith (University of St Andrews, St Andrews, U.K.), and S. J. Conway (University of Oxford, Oxford, U.K.)] (T.R. and M.D.E.), by a BBSRC grant (A.R.) [BB/H017917/1 awarded to I.R.B., J. H. Naismith, and O. Schiemann (University of St Andrews)], by a

DOI: 10.1021/acs.biochem.5b00294
Biochemistry 2015, 54, 4519−4530

Leverhulme Emeritus Fellowship (EM-2012-060\2), and by a CEMI grant to I.R.B. from the California Institute of Technology. The research leading to these results has received funding from the European Union Seventh Framework Programme (FP7/2007-2013 FP7/2007-2011) under Grant PITN-GA-2011-289384 (FP7-PEOPLE-2011-ITN NICHE) (H.G.) (awarded to S.M.).

Notes

The authors declare no competing financial interest.

■ ACKNOWLEDGMENTS

We thank Jim Naismith and his group (University of St Andrews) and Doug Rees (California Institute of Technology) for helpful discussions.

■ REFERENCES

(1) Berrier, C., Coulombe, A., Szabo, I., Zoratti, M., and Ghazi, A. (1992) Gadolinium Ion Inhibits Loss of Metabolites Induced by Osmotic Shock and Large Stretch-Activated Channels in Bacteria. *Eur. J. Biochem. 206*, 559−565.

(2) Booth, I. R., Miller, S., Rasmussen, A., Rasmussen, T., and Edwards, M. D. (2008) Mechanosensitive channels: Their mechanisms and roles in preserving bacterial ultrastructure during adaptation to environmental change. In *Bacterial Physiology: A Molecular Approach* (El-Sharoud, W., Ed.) pp 73−96, Springer, Berlin.

(3) Martinac, B., Buechner, M., Delcour, A. H., Adler, J., and Kung, C. (1987) Pressure-sensitive ion channel in Escherichia coli. *Proc. Natl. Acad. Sci. U. S. A. 84*, 2297−2301.

(4) Naismith, J. H., and Booth, I. R. (2012) Bacterial mechanosensitive channels–MscS: evolution's solution to creating sensitivity in function. *Annu. Rev. Biophys. 41*, 157−177.

(5) Levina, N., Totemeyer, S., Stokes, N. R., Louis, P., Jones, M. A., and Booth, I. R. (1999) Protection of Escherichia coli cells against extreme turgor by activation of MscS and MscL mechanosensitive channels: identification of genes required for MscS activity. *EMBO J. 18*, 1730−1737.

(6) Haswell, E. S., and Meyerowitz, E. M. (2006) MscS-like proteins control plastid size and shape in Arabidopsis thaliana. *Curr. Biol. 16*, 1−11.

(7) Nakayama, Y., Fujiu, K., Sokabe, M., and Yoshimura, K. (2007) Molecular and electrophysiological characterization of a mechanosensitive channel expressed in the chloroplasts of Chlamydomonas. *Proc. Natl. Acad. Sci. U. S. A. 104*, 5883−5888.

(8) Nakayama, Y., Yoshimura, K., and Iida, H. (2012) Organellar mechanosensitive channels in fission yeast regulate the hypo-osmotic shock response. *Nat. Commun. 3*, 1020.

(9) Sukharev, S. (2002) Purification of the small mechanosensitive channel of Escherichia coli (MscS): the subunit structure, conduction, and gating characteristics in liposomes. *Biophys. J. 83*, 290−298.

(10) Sukharev, S. I., Blount, P., Martinac, B., Blattner, F. R., and Kung, C. (1994) A large-conductance mechanosensitive channel in E. coli encoded by mscL alone. *Nature 368*, 265−268.

(11) Booth, I. R., Miller, S., Muller, A., and Lehtovirta-Morley, L. (2015) The evolution of bacterial mechanosensitive channels. *Cell Calcium 57*, 140−150.

(12) Bass, R. B., Strop, P., Barclay, M., and Rees, D. C. (2002) Crystal structure of Escherichia coli MscS, a voltage-modulated and mechanosensitive channel. *Science 298*, 1582−1587.

(13) Edwards, M. D., Li, Y., Kim, S., Miller, S., Bartlett, W., Black, S., Dennison, S., Iscla, I., Blount, P., Bowie, J. U., and Booth, I. R. (2005) Pivotal role of the glycine-rich TM3 helix in gating the MscS mechanosensitive channel. *Nat. Struct. Mol. Biol. 12*, 113−119.

(14) Miller, S., Bartlett, W., Chandrasekaran, S., Simpson, S., Edwards, M., and Booth, I. R. (2003) Domain organization of the MscS mechanosensitive channel of Escherichia coli. *EMBO J. 22*, 36−46.

(15) Rasmussen, T., Edwards, M. D., Black, S. S., Rasmussen, A., Miller, S., and Booth, I. R. (2010) Tryptophan in the pore of the mechanosensitive channel MscS: assessment of pore conformations by fluorescence spectroscopy. *J. Biol. Chem. 285*, 5377−5384.

(16) Reuter, M., Hayward, N. J., Miller, S., Dryden, D. T. F., and Booth, I. R. (2010) Hypo-osmotic shock: Does life end with a bang or a whimper? Individuality in bacterial cells. Manuscript in preparation.

(17) Sotomayor, M., and Schulten, K. (2004) Molecular dynamics study of gating in the mechanosensitive channel of small conductance MscS. *Biophys. J. 87*, 3050−3065.

(18) Steinbacher, S., Bass, R., Strop, P., and Rees, D. C. (2007) Structures of the prokaryotic mechanosensitive channels MscL and MscS. *Current Topics in Mechanosensitive Ion Channels, Part A 58*, 1−24.

(19) Wang, W., Black, S. S., Edwards, M. D., Miller, S., Morrison, E. L., Bartlett, W., Dong, C., Naismith, J. H., and Booth, I. R. (2008) The structure of an open form of an E. coli mechanosensitive channel at 3.45 A resolution. *Science 321*, 1179−1183.

(20) Rasmussen, A., Rasmussen, T., Edwards, M. D., Schauer, D., Schumann, U., Miller, S., and Booth, I. R. (2007) The Role of Tryptophan Residues in the Function and Stability of the Mechanosensitive Channel MscS from Escherichia coli. *Biochemistry 46*, 10899−10908.

(21) Lai, J. Y., Poon, Y. S., Kaiser, J. T., and Rees, D. C. (2013) Open and shut: crystal structures of the dodecylmaltoside solubilized mechanosensitive channel of small conductance from Escherichia coli and Helicobacter pylori at 4.4 and 4.1 A resolutions. *Protein science: a publication of the Protein Society 22*, 502−509.

(22) Zhang, X., Wang, J., Feng, Y., Ge, J., Li, W., Sun, W., Iscla, I., Yu, J., Blount, P., Li, Y., and Yang, M. (2012) Structure and molecular mechanism of an anion-selective mechanosensitive channel of small conductance. *Proc. Natl. Acad. Sci. U. S. A. 109*, 18180−18185.

(23) Edwards, M. D., Black, S., Rasmussen, T., Rasmussen, A., Stokes, N. R., Stephen, T. L., Miller, S., and Booth, I. R. (2012) Characterization of three novel mechanosensitive channel activities in Escherichia coli. *Channels 6*, 272−281.

(24) Schumann, U., Edwards, M. D., Rasmussen, T., Bartlett, W., van West, P., and Booth, I. R. (2010) YbdG in Escherichia coli is a threshold-setting mechanosensitive channel with MscM activity. *Proc. Natl. Acad. Sci. U. S. A. 107*, 12664−12669.

(25) Anishkin, A., Kamaraju, K., and Sukharev, S. (2008) Mechanosensitive channel MscS in the open state: modeling of the transition, explicit simulations, and experimental measurements of conductance. *J. Gen. Physiol. 132*, 67−83.

(26) Vasquez, V., Sotomayor, M., Marien Cortes, D., Roux, B., Schulten, K., and Perozo, E. (2008) Three-dimensional architecture of membrane-embedded MscS in the closed conformation. *J. Mol. Biol. 378*, 55−70.

(27) Vora, T., Corry, B., and Chung, S. H. (2006) Brownian dynamics investigation into the conductance state of the MscS channel crystal structure. *Biochim. Biophys. Acta, Biomembr. 1758*, 730−737.

(28) Anishkin, A., and Sukharev, S. (2004) Water dynamics and dewetting transitions in the small mechanosensitive channel MscS. *Biophys. J. 86*, 2883−2895.

(29) Beckstein, O., and Sansom, M. S. (2004) The influence of geometry, surface character, and flexibility on the permeation of ions and water through biological pores. *Phys. Biol. 1*, 42−52.

(30) Gandhi, C. S., Loots, E., and Isacoff, E. Y. (2000) Reconstructing voltage sensor-pore interaction from a fluorescence scan of a voltage-gated K+ channel. *Neuron 27*, 585−595.

(31) Han, X., Wang, C. T., Bai, J., Chapman, E. R., and Jackson, M. B. (2004) Transmembrane segments of syntaxin line the fusion pore of Ca2+-triggered exocytosis. *Science 304*, 289−292.

(32) Irizarry, S. N., Kutluay, E., Drews, G., Hart, S. J., and Heginbotham, L. (2002) Opening the KcsA K+ channel: tryptophan scanning and complementation analysis lead to mutants with altered gating. *Biochemistry 41*, 13653−13662.

(33) Muroi, Y., Arcisio-Miranda, M., Chowdhury, S., and Chanda, B. (2010) Molecular determinants of coupling between the domain III

DOI: 10.1021/acs.biochem.5b00294
Biochemistry 2015, 54, 4519−4530

voltage sensor and pore of a sodium channel. *Nat. Struct. Mol. Biol. 17*, 230−237.
(34) Ueno, S., Lin, A., Nikolaeva, N., Trudell, J. R., Mihic, S. J., Harris, R. A., and Harrison, N. L. (2000) Tryptophan scanning mutagenesis in TM2 of the GABA(A) receptor alpha subunit: effects on channel gating and regulation by ethanol. *Br. J. Pharmacol. 131*, 296−302.
(35) Booth, I. R., Edwards, M. D., Black, S., Schumann, U., Bartlett, W., Rasmussen, T., Rasmussen, A., and Miller, S. (2007) Physiological Analysis of Bacterial Mechanosensitive Channels. In *Methods in Enzymology* (Sies, M., and Haeussinger, D., Eds.) pp 47−61, Elsevier, Amsterdam.
(36) Bartlett, J. L., Levin, G., and Blount, P. (2004) An in vivo assay identifies changes in residue accessibility on mechanosensitive channel gating. *Proc. Natl. Acad. Sci. U. S. A. 101*, 10161−10165.
(37) Booth, I. R. (2014) Bacterial mechanosensitive channels: progress towards an understanding of their roles in cell physiology. *Curr. Opin. Microbiol. 18*, 16−22.
(38) Blount, P., Sukharev, S. I., Schroeder, M. J., Nagle, S. K., and Kung, C. (1996) Single residue substitutions that change the gating properties of a mechanosensitive channel in Escherichia coli. *Proc. Natl. Acad. Sci. U. S. A. 93*, 11652−11657.
(39) Carney, J., East, J. M., Mall, S., Marius, P., Powl, A. M., Wright, J. N., and Lee, A. G. (2006) Fluorescence quenching methods to study lipid-protein interactions. In *Current Protocols in Protein Science* (Coligan, J. E., et al., Eds.) Chapter 19, Unit 19.12, Wiley, New York, DOI: 10.1002/0471142301.ps1912s45.
(40) Markwell, M. A., Haas, S. M., Bieber, L. L., and Tolbert, N. E. (1978) A modification of the Lowry procedure to simplify protein determination in membrane and lipoprotein samples. *Anal. Biochem. 87*, 206−210.
(41) Ladokhin, A. S., Jayasinghe, S., and White, S. H. (2000) How to measure and analyze tryptophan fluorescence in membranes properly, and why bother? *Anal. Biochem. 285*, 235−245.
(42) Heuberger, E. H., Veenhoff, L. M., Duurkens, R. H., Friesen, R. H., and Poolman, B. (2002) Oligomeric state of membrane transport proteins analyzed with blue native electrophoresis and analytical ultracentrifugation. *J. Mol. Biol. 317*, 591−600.
(43) Booth, I. R., Edwards, M. D., Black, S., Schumann, U., Bartlett, W., Rasmussen, T., Rasmussen, A., and Miller, S. (2007) Physiological analysis of bacterial mechanosensitive channels. *Methods Enzymol. 428*, 47−61.
(44) Booth, I. R., Edwards, M. D., Black, S., Schumann, U., and Miller, S. (2007) Mechanosensitive channels in bacteria: signs of closure? *Nat. Rev. Microbiol. 5*, 431−440.
(45) Li, Y., Wray, R., and Blount, P. (2004) Intragenic suppression of gain-of-function mutations in the Escherichia coli mechanosensitive channel, MscL. *Mol. Microbiol. 53*, 485−495.
(46) Lakowicz, J. R. (2006) *Principles of Fluorescence Spectroscopy*, 3rd ed., Springer, New York.
(47) Tallmadge, D. H., Huebner, J. S., and Borkman, R. F. (1989) Acrylamide quenching of tryptophan photochemistry and photophysics. *Photochem. Photobiol. 49*, 381−386.
(48) Vivian, J. T., and Callis, P. R. (2001) Mechanisms of tryptophan fluorescence shifts in proteins. *Biophys. J. 80*, 2093−2109.
(49) Vasquez, V., Sotomayor, M., Cordero-Morales, J., Schulten, K., and Perozo, E. (2008) A structural mechanism for MscS gating in lipid bilayers. *Science 321*, 1210−1214.
(50) Harris, D. C. (2010) Applications of Spectrophotometry. In *Quantitative Chemical Analysis*, 8th ed., pp 419−444, W. H. Freeman & Co., New York.
(51) Weber, G. (1960) Fluorescence-polarization spectrum and electronic-energy transfer in tyrosine, tryptophan and related compounds. *Biochem. J. 75*, 335−345.
(52) Weber, G., and Shinitzky, M. (1970) Failure of Energy Transfer between Identical Aromatic Molecules on Excitation at the Long Wave Edge of the Absorption Spectrum. *Proc. Natl. Acad. Sci. U. S. A. 65*, 823−830.
(53) Wu, P., and Brand, L. (1994) Resonance energy transfer: methods and applications. *Anal. Biochem. 218*, 1−13.
(54) Clegg, R. M. (1995) Fluorescence resonance energy transfer. *Curr. Opin. Biotechnol. 6*, 103−110.
(55) Ward, R., Pliotas, C., Branigan, E., Hacker, C., Rasmussen, A., Hagelueken, G., Booth, I. R., Miller, S., Lucocq, J., Naismith, J. H., and Schiemann, O. (2014) Probing the structure of the mechanosensitive channel of small conductance in lipid bilayers with pulsed electron-electron double resonance. *Biophys. J. 106*, 834−842.
(56) Pliotas, C., Ward, R., Branigan, E., Rasmussen, A., Hagelueken, G., Huang, H., Black, S. S., Booth, I. R., Schiemann, O., and Naismith, J. H. (2012) Conformational state of the MscS mechanosensitive channel in solution revealed by pulsed electron-electron double resonance (PELDOR) spectroscopy. *Proc. Natl. Acad. Sci. U. S. A. 109*, E2675−2682.
(57) Okada, K., Moe, P. C., and Blount, P. (2002) Functional design of bacterial mechanosensitive channels. Comparisons and contrasts illuminated by random mutagenesis. *J. Biol. Chem. 277*, 27682−27688.
(58) Powl, A. M., Wright, J. N., East, J. M., and Lee, A. G. (2005) Identification of the hydrophobic thickness of a membrane protein using fluorescence spectroscopy: studies with the mechanosensitive channel MscL. *Biochemistry 44*, 5713−5721.
(59) Powl, A. M., East, J. M., and Lee, A. G. (2005) Heterogeneity in the binding of lipid molecules to the surface of a membrane protein: hot spots for anionic lipids on the mechanosensitive channel of large conductance MscL and effects on conformation. *Biochemistry 44*, 5873−5883.
(60) Powl, A. M., East, J. M., and Lee, A. G. (2003) Lipid-protein interactions studied by introduction of a tryptophan residue: The mechanosensitive channel MscL. *Biochemistry 42*, 14306−14317.
(61) Clackson, T., Ultsch, M. H., Wells, J. A., and de Vos, A. M. (1998) Structural and functional analysis of the 1:1 growth hormone:receptor complex reveals the molecular basis for receptor affinity. *J. Mol. Biol. 277*, 1111−1128.
(62) Powl, A. M., Carney, J., Marius, P., East, J. M., and Lee, A. G. (2005) Lipid interactions with bacterial channels: fluorescence studies. *Biochem. Soc. Trans. 33*, 905−909.
(63) Chiang, C. S., Shirinian, L., and Sukharev, S. (2005) Capping transmembrane helices of MscL with aromatic residues changes channel response to membrane stretch. *Biochemistry 44*, 12589−12597.
(64) Killian, J. A., and von Heijne, G. (2000) How proteins adapt to a membrane-water interface. *Trends Biochem. Sci. 25*, 429−434.
(65) Ramachandran, G. N., Ramakrishnan, C., and Sasisekharan, V. (1963) Stereochemistry of polypeptide chain configurations. *J. Mol. Biol. 7*, 95−99.
(66) Bass, R. B., Strop, P., Barclay, M., and Rees, D. C. (2002) Crystal structure of Escherichia coli MscS, a voltage-modulated and mechanosensitive channel. *Science 298*, 1582−1587.
(67) Sobolev, V., Wade, R. C., Vriend, G., and Edelman, M. (1996) Molecular docking using surface complementarity. *Proteins: Struct., Funct., Genet. 25*, 120−129.
(68) Blount, P., Schroeder, M. J., and Kung, C. (1997) Mutations in a bacterial mechanosensitive channel change the cellular response to osmotic stress. *J. Biol. Chem. 272*, 32150−32157.
(69) Booth, I. R., and Blount, P. (2012) The MscS and MscL families of mechanosensitive channels act as microbial emergency release valves. *J. Bacteriol. 194*, 4802−4809.

DOI: 10.1021/acs.biochem.5b00294
Biochemistry 2015, 54, 4519−4530